Supporting Information for

Probing the electronic properties of the electrified silicon/water interface by combining simulations and experiments

Author Information

Affiliations

Pritzker School of Molecular Engineering, The University of Chicago, Chicago, Illinois, 60637, USA

Zifan Ye & Giulia Galli

Department of Chemistry, The University of Chicago, Chicago, Illinois, 60637, USA

Aleksander Prominski, Bozhi Tian & Giulia Galli

Materials Science Division, Argonne National Laboratory, Lemont, Illinois, 60439, USA

Giulia Galli

Supplementary Note 1. Electric field intensities and band edge positions for electrified H-Si/water interfaces.

Table S1: The intensities of electric field applied to the H-Si/water interface in this study and the corresponding built-in potentials. The electric field was determined based on the thickness of the intrinsic layer (~150nm) of the experimental PIN-Si structure,(1) and the built-in voltage across a Si p-n diode junction (~ 0.7 V) (2). We also considered smaller electric fields relevant to the electronic properties of Si-based bioelectronic devices.

Electric field / a.u	Voltage / V
0	0
4.5×10^{-6}	0.35
7.0×10^{-6}	0.54
9.5×10^{-6}	0.73

Figure S1: Computed valence band maximum (VBM) and conduction band minimum (CBM) of water interfaced with a H-Si(100) sample, as a function of the applied electric field. The VBM and CBM were computed at the PBE level(3) of density functional theory on trajectories generated using first principles molecular dynamics and were corrected using the G_0W_0 approximation.(4) The band gap of Si is slightly larger than that obtained at the same level of theory of bulk Si due to the use of a slab with a limited number of layers.

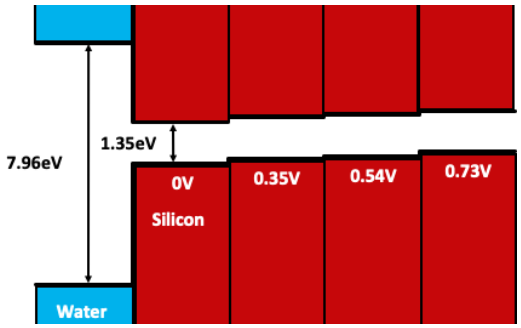

Table S2: Valence band maximum (VBM) and conduction band minimum (CBM) of the hydrogenated Si(100) surface interfaced with water, as a function of the applied electric field; the values were calculated using density functional theory and the PBE functional(3) and corrected using the with G_0W_0 approximation.

	DFT		G_0W_0	
Voltage/ V	VBM/eV	CBM/eV	VBM/eV	CBM/eV
0	-3.80	-4.55	-5.05	-3.70
0.35	-3.67	-4.42	-4.92	-3.57
0.54	-3.58	-4.33	-4.83	-3.48
0.73	-3.43	-4.18	-4.68	-3.33

Supplementary Note 2. Flat-band potentials at point of zero conditions

Table S3: The computed flat-band potential U_{fb} of different electrified samples; the V_{dip} and E_F were obtained from band alignment calculations. V_{dip} is the electrostatic potential difference between electrified and non-electrified Si(100)/Water structure. The E_F is determined as the midpoint between the CBM and VBM. Since the band edge positions were computed in the presence of water molecules, solvation effects are included.

Unit: eV

Voltage /V	V_{dip}	E_F	U_{fb} vs. vacuum
0	0	-4.37	-4.37
0.35	0.129	-4.25	-4.12
0.54	0.224	-4.15	-3.93
0.73	0.368	-4.00	-3.64

Supplementary Note 3. Tunneling current images

Figure S2: Computed tunneling current images (see main text) for a bias voltage -1eV for non-electrified (a) and electrified (b,c) samples. In (b) and (c) the voltage applied to the interface is 0.35V, and 0.67V, respectively. The area and position for high current density regions is the same for electrified and non-electrified samples; the maximum current value is slightly larger in electrified samples than in non-electrified ones.

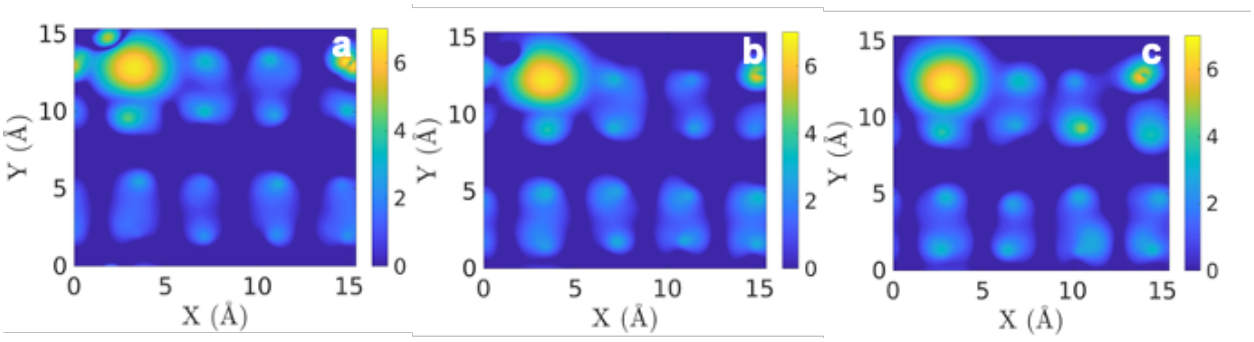

Supplementary Note 4. Bulk Si relaxed with the density functionals optB88 and PBE

Table S4. The lattice parameter of bulk Si relaxed with the van-der-Waals functional optB88 (5) and semi-local functional PBE (3). The lattice constant of bulk Si obtained with the PBE and optB88 functionals are compared with previous simulation results as well as with experimental values. The lattice constants obtained with PBE and opbB88 differ by ~ 0.1%.

Unit: Å

Functional	**Reference (6)**	**Present work**
optB88	5.460	5.450
PBE	5.466	5.456
Exp.(6)		5.416

Supplementary Note 5. Dipole moment of water molecules in liquid water

We conducted first principles molecular dynamics (FPMD) simulations with van der Walls density functional optB88(5) at 330K and PBE at 400K. The two temperature were chosen to correct for inaccuracies of the two functionals in modeling the structure of water (See Ref. (7) and (8) for optB88 and PBE, respectively). To analyze the structural properties of interfacial water, we computed the molecular dipole moment of water using maximally localized Wannier functions.(9) A comparison of the results of the two functionals is presented in Fig. S3 and S4 showing similar results.

Figure S3. The probability distribution of molecular dipole moment of water obtained for PBE and optB88 equilibrated samples. The simulations were conducted with 124 water molecules and the BDP thermostat. When using PBE, the average dipole moment of water molecules is ~ 2.93D, slightly smaller than that of the bulk PBE water ~ 3.06D by 4.2%. Such a decrease has been previously observed close to surfaces and under confinement.(10) The average dipole moment of water molecules calculated with the optB88 functional (~ 2.88D) is slightly smaller than the PBE one, yet similar (1.7% difference), again consistent with previous reports.(7) The decrease relative to the optB88 bulk values ~ 3.00D is 4.0%, similar to the decrease 4.2% found in the PBE case.

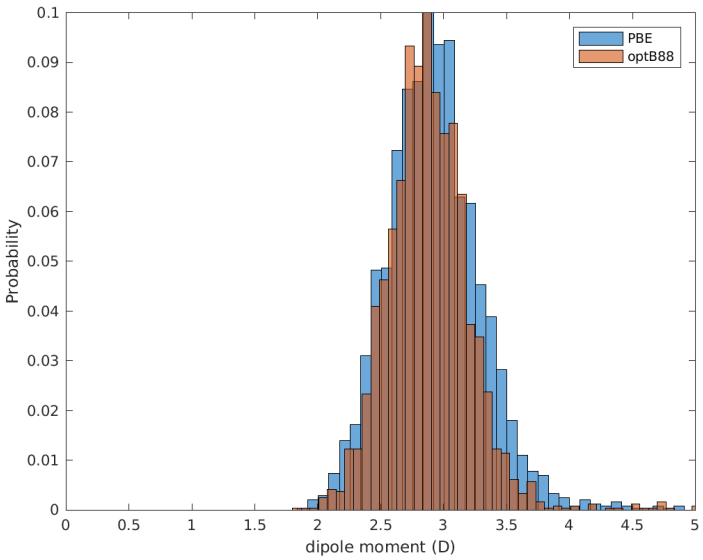

Figure S4. Molecular dipole moment (D) of water molecules in bulk and interfacial regions (within 5Å from the surface) of a simulation conducted with 124 water molecules using PBE and optB88 equilibrated samples. When using the PBE functional, we find that water molecules in the bulk region show a slightly larger dipole moment compared with those in the interfacial region, (2.95D vs. 2.87D). When using the optB88 functional, we find the same the trend: water molecules in the bulk region have a larger dipole than the interfacial region (2.89D vs. 2.85D). Comparing quantitatively the PBE and optB88 results, we find that the reduction of dipole moment from the bulk to the interfacial region is slightly more significant for PBE (~2.7%) than optB88 water (~1.4%).

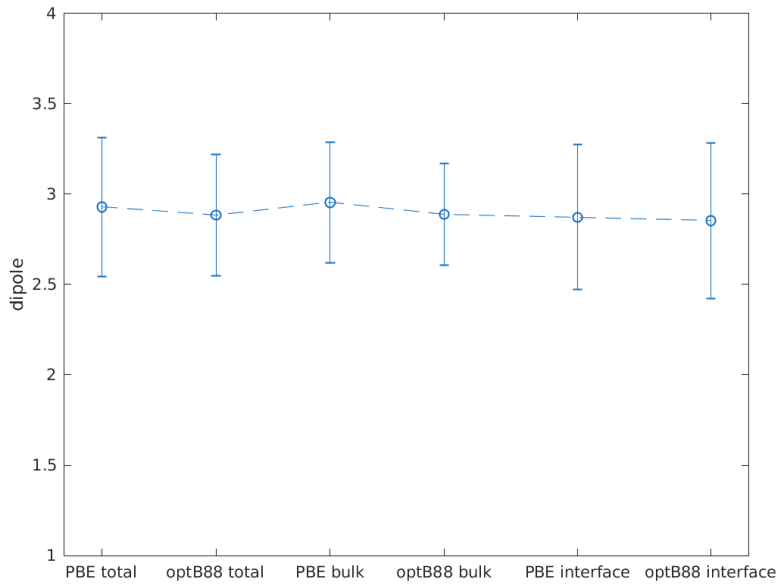

From the comparison presented above we deemed PBE sufficiently accurate for the scope of the analysis of interest to our paper and carried out simulations under bias using the PBE functional.

Supplementary Note 6. Equilibration of interfacial samples

We equilibrated and collected FPMD trajectories for pristine and electrified samples for ~ 10 and 5ps, respectively. We checked the equilibration process by monitoring whether the total energy of the system fluctuated at a stable value and whether the system temperatures reached the target. We also calculated the equipartition of energy between different species to verify the equilibration process, as shown in Fig. S5.

Figure S5. Normalized probability distribution of temperature (in terms of squared velocity) of individual species of the FPMD with a thermostat set to 400K for PBE functional. The average temperature for H, O and Si atoms are all reached the target temperature of 400K.

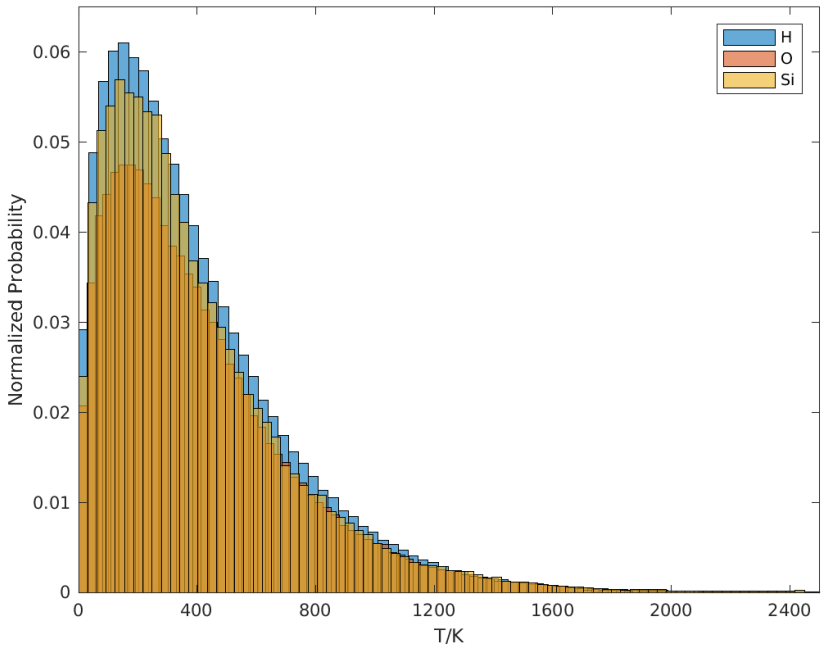

References

1. Y. Jiang *et al.*, Rational design of silicon structures for optically controlled multiscale biointerfaces. *Nature biomedical engineering* **2**, 508-521 (2018).
2. Y. Jiang, B. Tian, Inorganic semiconductor biointerfaces. *Nature Reviews Materials* **3**, 473-490 (2018).
3. J. P. Perdew, K. Burke, M. Ernzerhof, Generalized gradient approximation made simple. *Physical review letters* **77**, 3865 (1996).
4. T. Anh Pham *et al.*, Band offsets and dielectric properties of the amorphous Si3N4/Si (100) interface: A first-principles study. *Applied Physics Letters* **102**, 241603 (2013).
5. J. Klimeš, D. R. Bowler, A. Michaelides, Chemical accuracy for the van der Waals density functional. *Journal of Physics: Condensed Matter* **22**, 022201 (2009).
6. J. Klimeš, D. R. Bowler, A. Michaelides, Van der Waals density functionals applied to solids. *Physical Review B* **83**, 195131 (2011).
7. C. Zhang, J. Wu, G. Galli, F. Gygi, Structural and vibrational properties of liquid water from van der Waals density functionals. *Journal of chemical theory and computation* **7**, 3054-3061 (2011).
8. M. D. LaCount, F. Gygi, Ensemble first-principles molecular dynamics simulations of water using the SCAN meta-GGA density functional. *The Journal of chemical physics* **151**, 164101 (2019).
9. F. Gygi, J.-L. Fattebert, E. Schwegler, Computation of maximally localized Wannier functions using a simultaneous diagonalization algorithm. *Computer physics communications* **155**, 1-6 (2003).
10. V. Rozsa, T. A. Pham, G. Galli, Molecular polarizabilities as fingerprints of perturbations to water by ions and confinement. *The Journal of chemical physics* **152**, 124501 (2020).